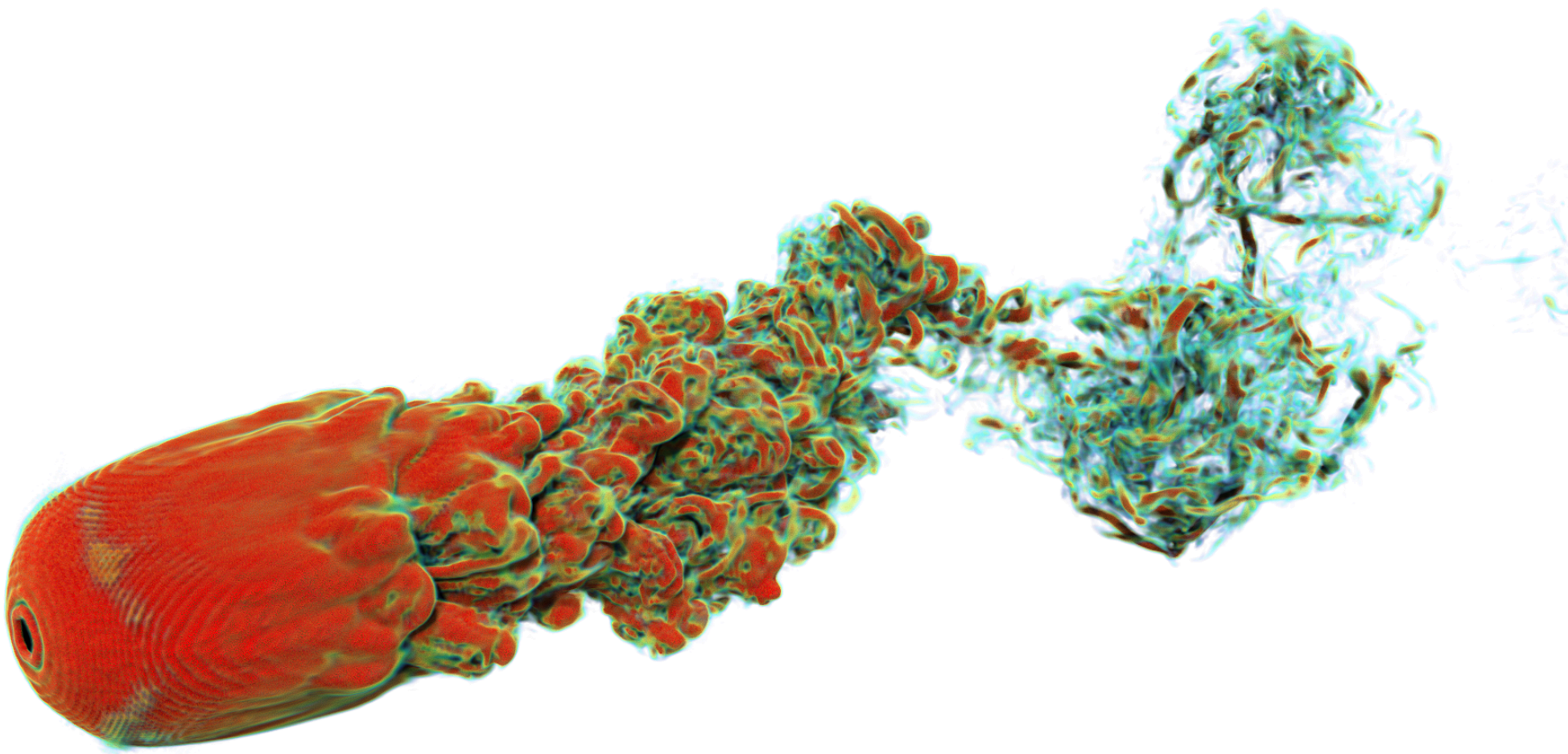


nTop Fluids Examples With Focus on Scale-Resolving Flows



Dr.-Ing. Marc Haußmann
Dr.-Ing. Max Gaedtke
Jonathan Jeppener-Haltenhoff
Florian Raichle
Arjun Rachith

Contents

This document contains the numerical results of nTop Fluids, a GPU-native implementation of the Lattice Boltzmann Method (LBM), applied to various complex flow problems. The results are presented alongside publicly available experimental data referenced at the end of this document.

Test case 1: Flow over a sphere	3
Test case 2: Volvo flame holder	5
Test case 3: High-lift airfoil	8
Test case 4: Automotive side mirror.	10
Test case 5: FDA nozzle	12
References	14

Test case 1: Flow over a sphere

The flow over a sphere is used extensively in external aerodynamics to study and understand the principles of drag, flow separation, boundary layer behavior, and wake dynamics. This case is crucial in validating computational methods and experimental techniques used in aerodynamic analysis. The Reynolds number of the flow is defined as:

$$\text{Re}_\infty = \frac{u_\infty D}{\nu},$$

where u_∞ is the freestream velocity, D is the sphere diameter and ν is the kinematic viscosity. The geometrical dimensions for the simulation domain are shown in Figure 1.

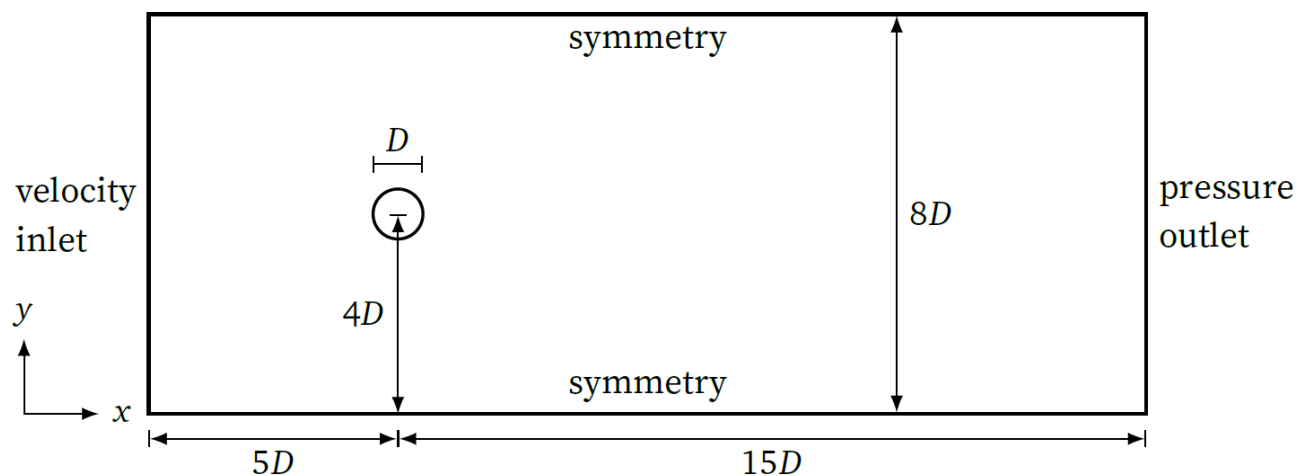


Figure 1: Geometrical dimensions of the flow over sphere test case

Steady-state laminar wake at $\text{Re}_\infty = 100$

At a Reynolds number of 100, the flow over a sphere is in the laminar regime, characterized by smooth, orderly flow patterns around the sphere. The boundary layer remains attached to the sphere's surface for a significant portion of the circumference before separating. Flow separation occurs near the rear of the sphere, leading to the formation of a steady and symmetric wake. The wake is relatively narrow and stable compared to higher Reynolds numbers, with two symmetric vortices forming just downstream of the sphere.

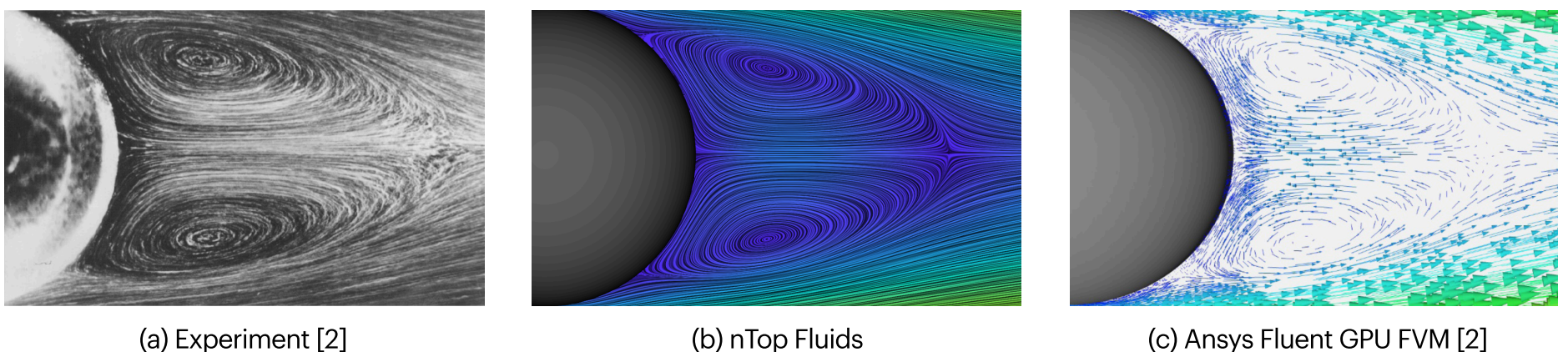


Figure 2: Laminar wake with a symmetric vortex pair at $\text{Re} = 100$

Both nTop and Ansys Fluent solvers successfully describe the emerging wake flow pattern behind a sphere, see Figure 2. The simulations from both solvers show vortex centers in the wake that are well-aligned and consistent with experimental observations. This agreement indicates that both computational tools are capable of accurately capturing the flow separation and vortex formation at the given Reynolds number, providing reliable insights to the wake dynamics.

Turbulent wake and vortex shedding at $Re_\infty = 1000$

The flow over a sphere at a $Re_\infty = 1000$ is characterized by a laminar boundary layer that separates from the sphere's surface before transitioning to turbulence. The separated flow results in a broad and complex wake with large-scale vortex structures. The wake is characterized by unsteady and chaotic flow patterns, with vortices shedding alternately from either side of the sphere.

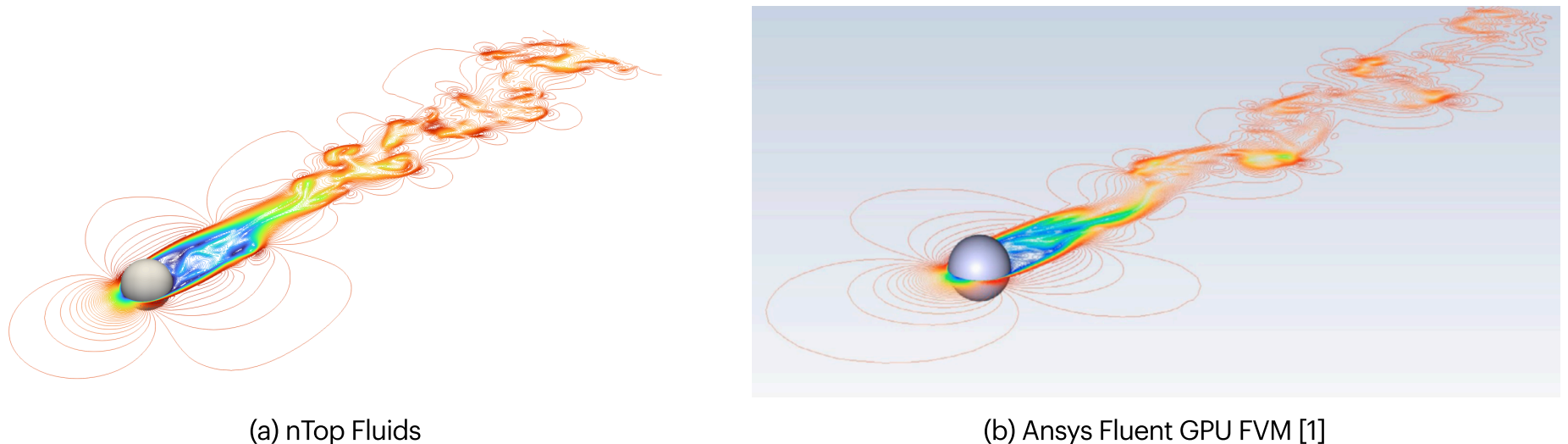


Figure 3: Depiction of the turbulent wake with vortex shedding at $Re_\infty = 1000$ using contours of the velocity magnitude

At a $Re_\infty = 1000$, nTop and Ansys Fluent solvers produce similar wake flow patterns behind the sphere, see Figure 3. The flow features a laminar boundary layer that separates from the sphere's surface, transitioning into a turbulent wake. Both solvers show a broad and complex wake with large-scale vortex structures. The unsteady and chaotic nature of the wake is well-represented, with alternating vortex shedding that is consistent between the two solvers. Aligning closely with experimental observations, both solvers are similarly capable of accurately modeling the transitional flow and turbulent wake dynamics at higher Reynolds numbers.

Drag coefficient comparison

The drag coefficient of a sphere is defined as

$$C_D = \frac{2F_D}{\rho u_\infty^2 \pi r^2},$$

where F_D is the drag force, ρ is the density of the fluid and r is the radius of the sphere. The drag was calculated using nTop across four orders of magnitude, ranging $Re_\infty = 10^1 \dots 10^4$, see Figure 4. At $Re_\infty = 100$, the nTop results show excellent agreement with Ansys Fluent [2, 1], with an error of less than two percent when compared to standard correlations. However, at $Re = 1000$, there is a slightly higher deviation from Fluent's results. This discrepancy is attributed to the smaller computational domain used in nTop due to the uniform grid, where boundary conditions have a stronger influence. Notably, nTop shows better results than other Lattice Boltzmann methods (LBM) that use a uniform grid [6], showcasing its superior capability of modeling non resolved boundary layer effects.

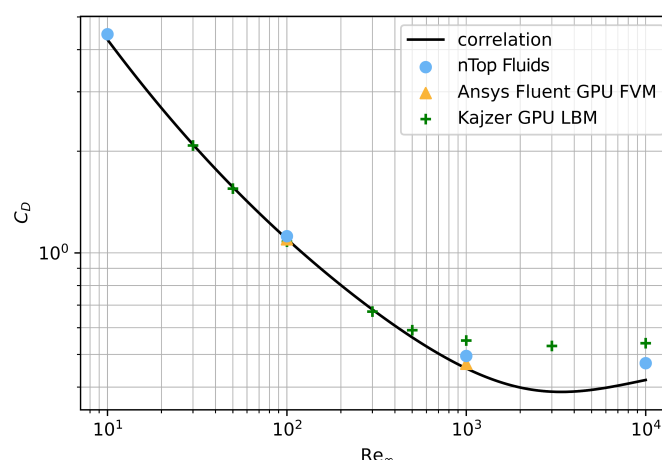


Figure 4: Drag coefficient C_D over Reynolds number Re_∞

Test case 2: Volvo flame holder

Another example problem to evaluate is the Volvo flame holder test [7]. This case involves analyzing a flow over a triangular bluff body situated within a rectangular channel to evaluate the model accuracy. The prism-shaped flame holder, placed in an air stream, exhibits several transient phenomena, such as vortex shedding, oscillating shear layers, and recirculation zones, which can only be accurately captured using scale-resolving turbulence models. The problem setup is depicted in Figure 5. The bulk Reynolds number of this case is defined as

$$\text{Re}_b = \frac{U_b D}{\nu} = 48000,$$

where U_b is the bulk velocity and D the bluff body length. Vertical lines downstream of the flame holder indicate stations where experimental data was recorded, providing reference points for validating the simulation results.

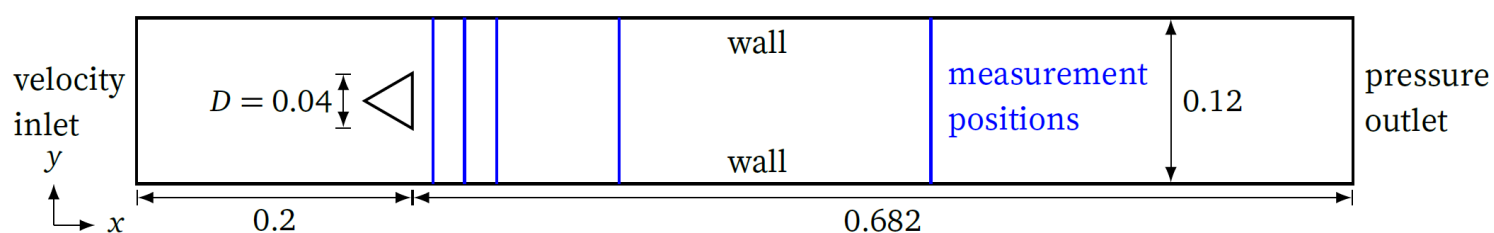
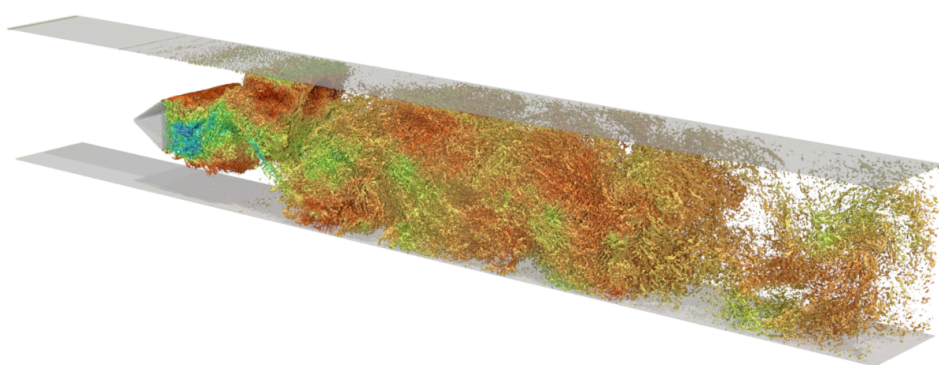
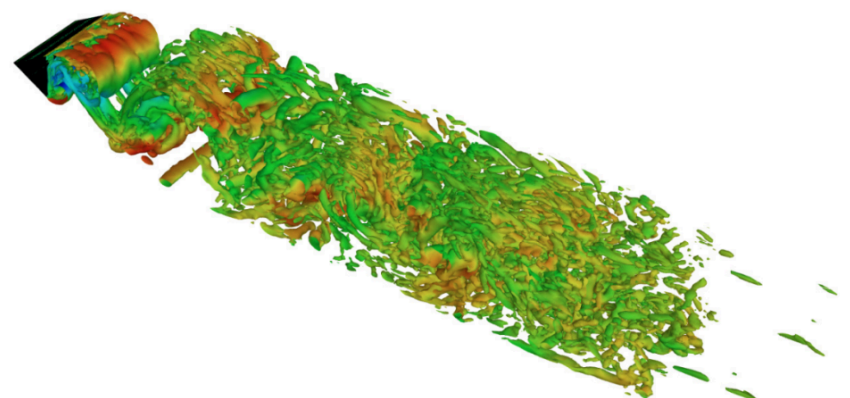


Figure 5: Geometrical dimensions of the Volvo flame holder test case



(a) nTop Fluids



(b) Ansys Fluent GPU FVM [2]

Figure 6: Isosurfaces of the Q-criterion colored by the velocity magnitude

First, a quantitative comparison of the wake flow patterns is conducted. nTop employs wall-modeled large eddy simulation (WM-LES) and ANSYS Fluent uses a hybrid RANS-LES approach. In Figure 6, this distinction is particularly evident when visualizing the flow using the Q-criterion, which identifies regions of rotational flow and highlights vortices. The Q-criterion visualization in nTop reveals a high density of smaller-scale vortices, indicating its capability in resolving complex, transient flow features such as vortex shedding and recirculation zones. This enhanced resolution provides a representation of the wake dynamics, showcasing nTop's effectiveness in scale-resolving turbulence modeling.

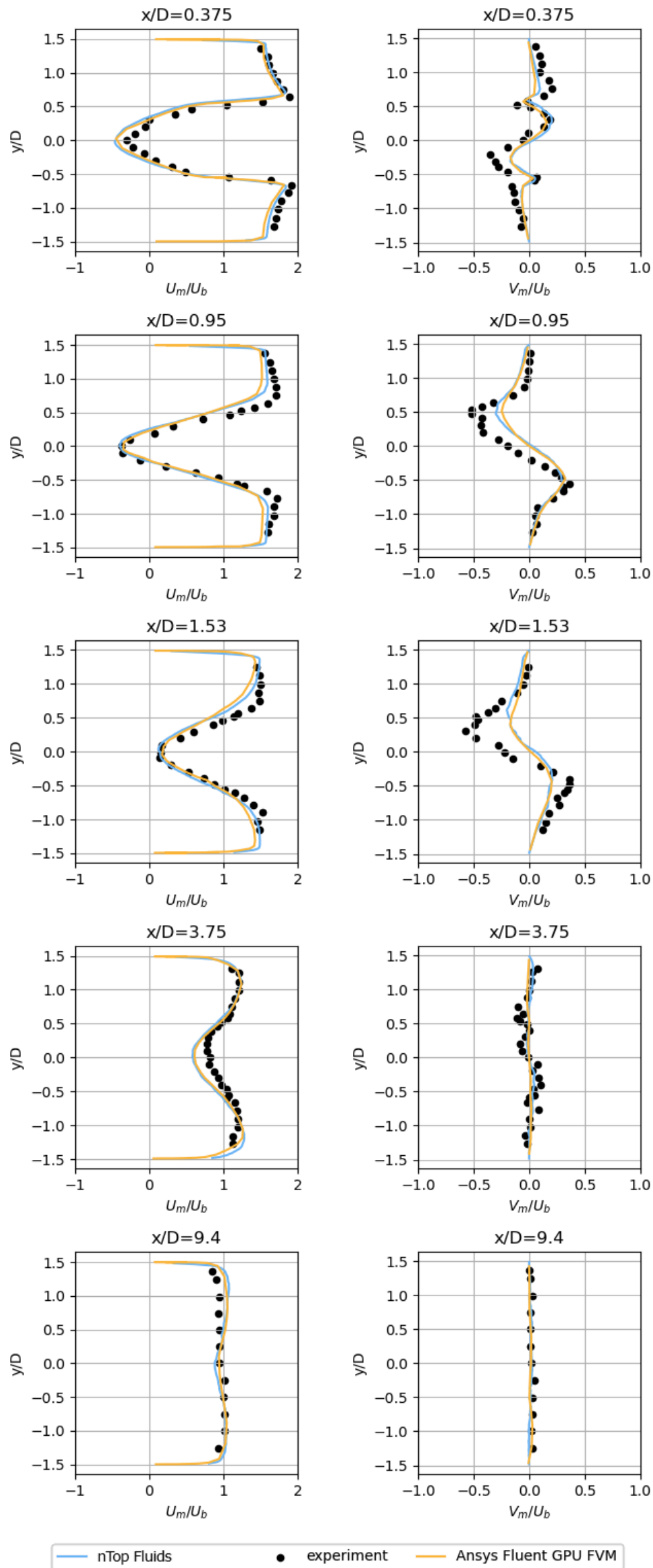


Figure 7: Normalized time-averaged axial and transverse velocities are plotted at predefined locations

Evaluating time-averaged velocity distributions, both nTop and Ansys Fluent show good agreement with the experimental reference solution. In Figure 7, normalized mean axial and transverse velocities are plotted at various locations in the wake of the bluff body ($x/D = 0.375, 0.95, 1.53, 3.75, \text{ and } 9.4$). These plots indicate that both CFD simulations agree well with experimental data across these locations and almost match each other. The good correlation in both axial and transverse velocity profiles demonstrates that nTop's WM-LES and Fluent's hybrid RANS-LES approaches are effective in capturing the mean flow characteristics of the wake. This validation against experimental results confirms the reliability of both solvers in accurately modeling the wake flow patterns behind the bluff body. It also shows that the FVM hybrid RANS-LES and LBM WM-LES methods lead to equivalent results.

Test case 3: High-lift airfoil

Evaluating the lift and drag characteristics of various airfoil designs has been essential for advancing aerodynamic performance. Numerous standard airfoil shapes have been extensively studied through both experimental methods and computational simulations. We focus on the well-documented NREL high-lift airfoil (S805), which has comprehensive experimental data available [8]. The used dimensions of the simulation domain for the nTop solver is depicted in Figure 8. The investigated chord Reynolds number is defined as

$$\text{Re}_c = \frac{u_\infty c}{\nu} = 10^6,$$

where c is the chord length of the airfoil. Both solvers perform a two-dimensional simulation. Ansys Fluent uses a $k-\omega$, SST RANS model, nTop utilizes a WM-LES.

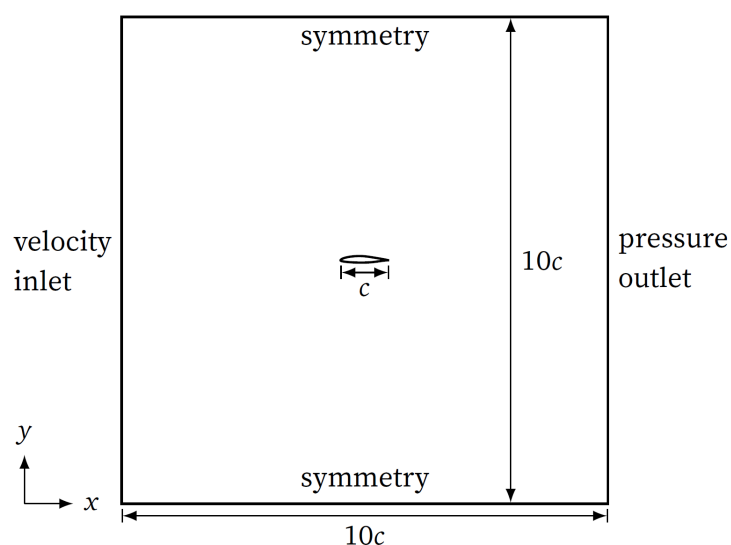


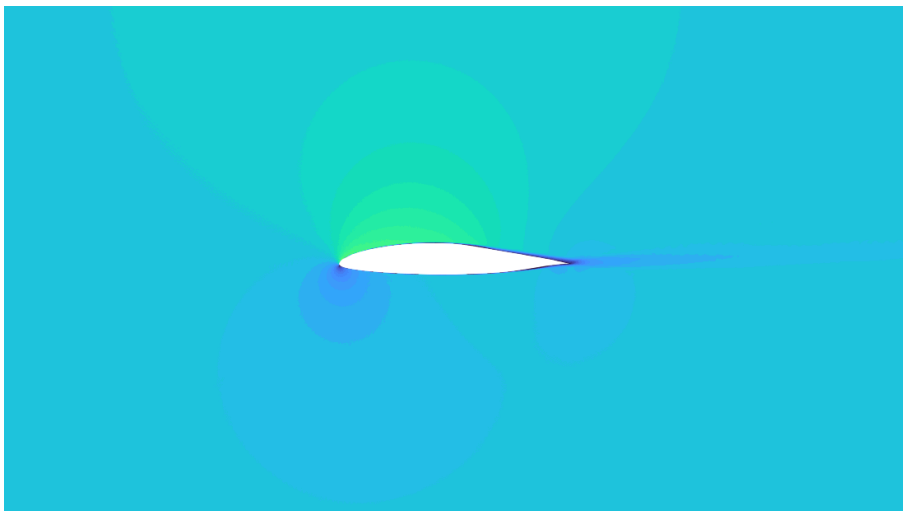
Figure 8: Geometrical dimensions of the high-lift airfoil test case

The time-averaged velocity contours for two angles of attack (AOA), 5 and 10 degrees, are compared for both solvers, see Figure 9. The results demonstrate that the separation point and the wake shape are remarkably similar between the two solvers. This similarity indicates that both solvers are accurately capturing the critical aerodynamic features, such as boundary layer behavior and vortex formation, validating the effectiveness of the computational models used in both nTop and Ansys Fluent for simulating high-lift airfoil performance.

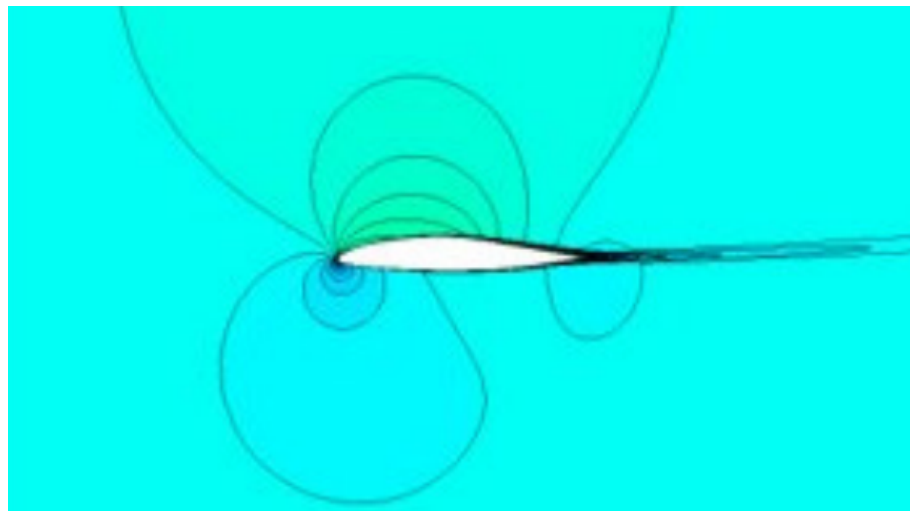
The lift coefficient of an airfoil is calculated as

$$C_L = \frac{2F_L}{\rho u_\infty^2 c},$$

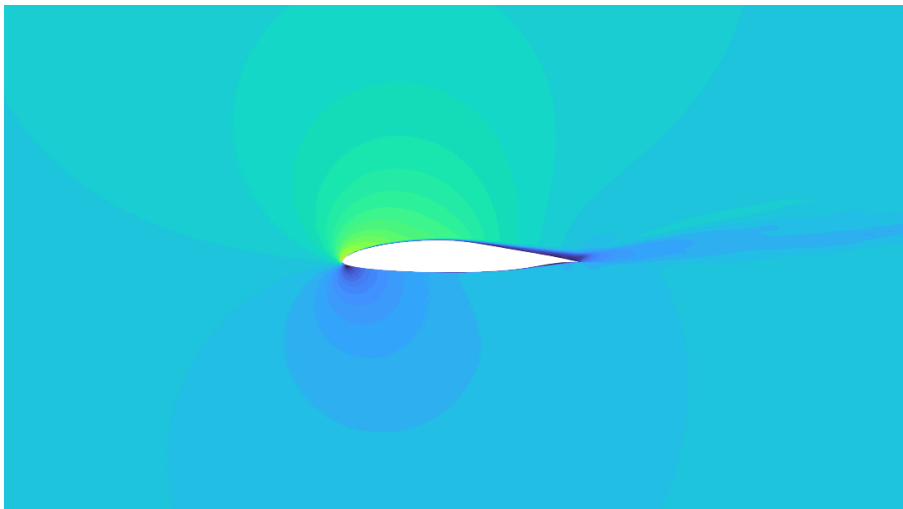
where F_L is the lift force. A quantitative comparison of the lift coefficient over different AOAs reveals that both solvers show similar trends when compared to experimental data, see Figure 10. At lower AOAs, the simulation results align well with experimental measurements, indicating that both solvers effectively capture the aerodynamic performance of the airfoil. However, as the AOA increases, deviations from experimental results become more noticeable. This divergence is particularly evident at higher AOAs, where the two-dimensional flow assumptions used in the simulations begin to break down, leading to inaccuracies in the modeling. This breakdown highlights the limitations of the two-dimensional simulation approach, as the flow becomes more three-dimensional and complex, affecting the accuracy of the lift predictions.



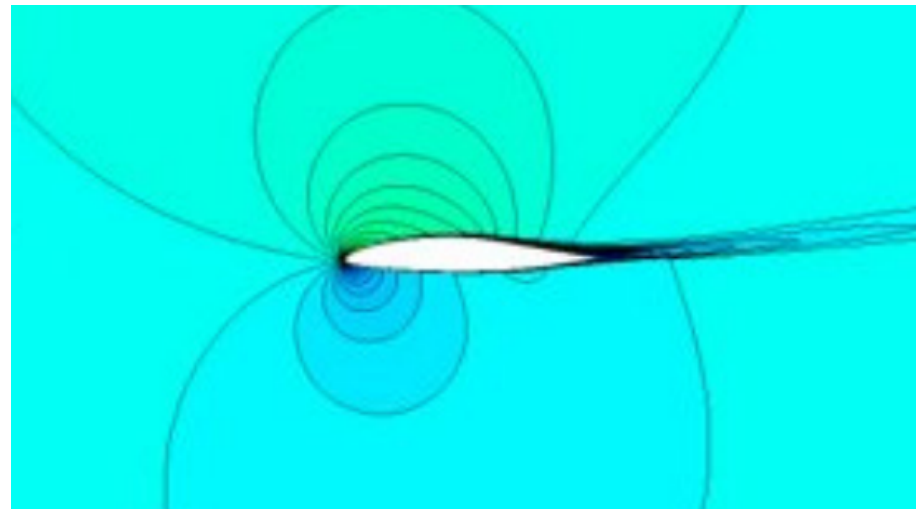
(a) nTop Fluids, AOA = 5°



(b) Ansys Fluent GPU FVM [2], AOA = 5°



(c) nTop Fluids, AOA = 10°



(d) Ansys Fluent GPU FVM [2], AOA = 10°

Figure 9: Time-averaged velocity contours for 5° and 10° angle of attack

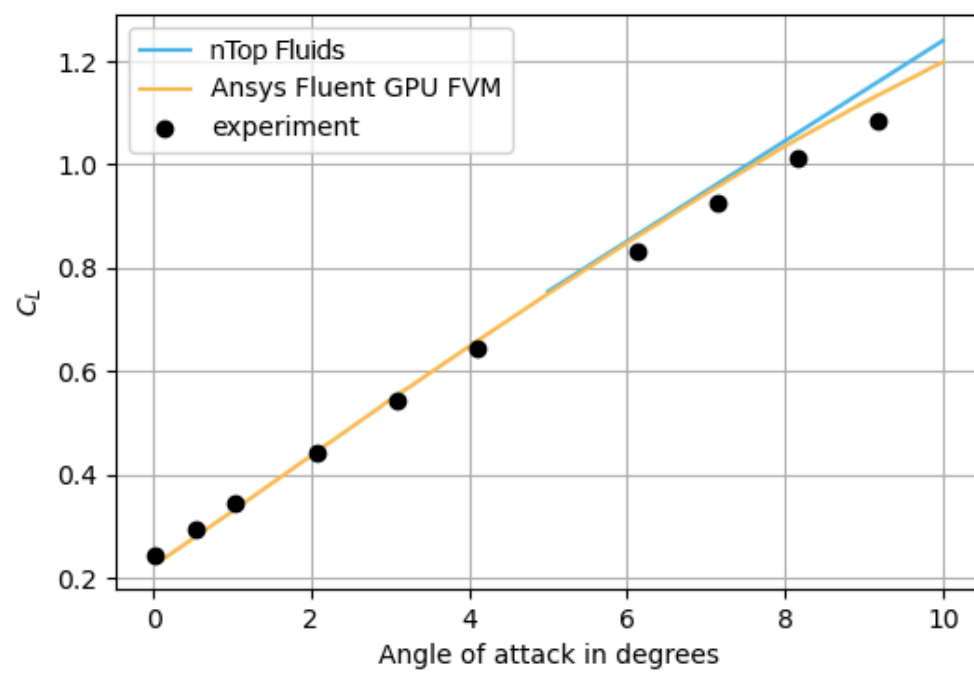


Figure 10: Lift coefficient C_L over angle of attack

Test case 4: Automotive side mirror

Automotive manufacturers have long aimed to improve aerodynamic performance and reduce cabin noise through optimized side mirror designs. Extensive experimental studies documented in the literature, such as the one of Hold et al. [4], provide valuable benchmarks for assessing simulation tools. The flow around a car's side mirror is complex, involving turbulent flow structures and pressure fluctuations that must be accurately simulated in a scale resolving simulation. In this context, Fluent employs a hybrid RANS-LES model and nTop utilizes a WM-LES approach. The dimensions of the used bounding box around the side mirror are depicted in Figure 11.

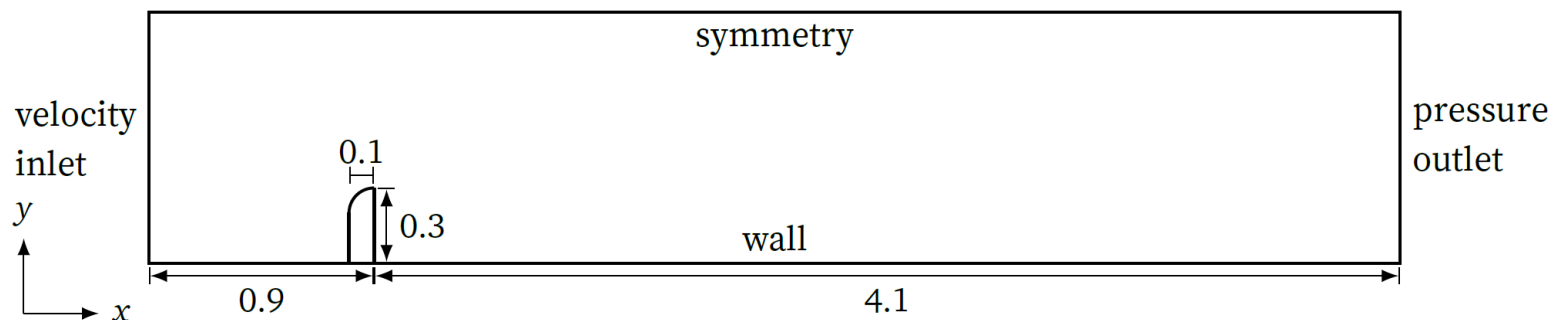


Figure 11: Geometrical dimensions of the generic side mirror test case

A qualitative comparison of the wake flow structures is displayed in Figure 12. It reveals that nTop exhibits smaller-scale vortex structures in the wake compared to Ansys Fluent. nTop's WM-LES results in a detailed depiction of the wake's intricate flow patterns. This includes smaller, more defined vortex structures and a more nuanced representation of turbulence.

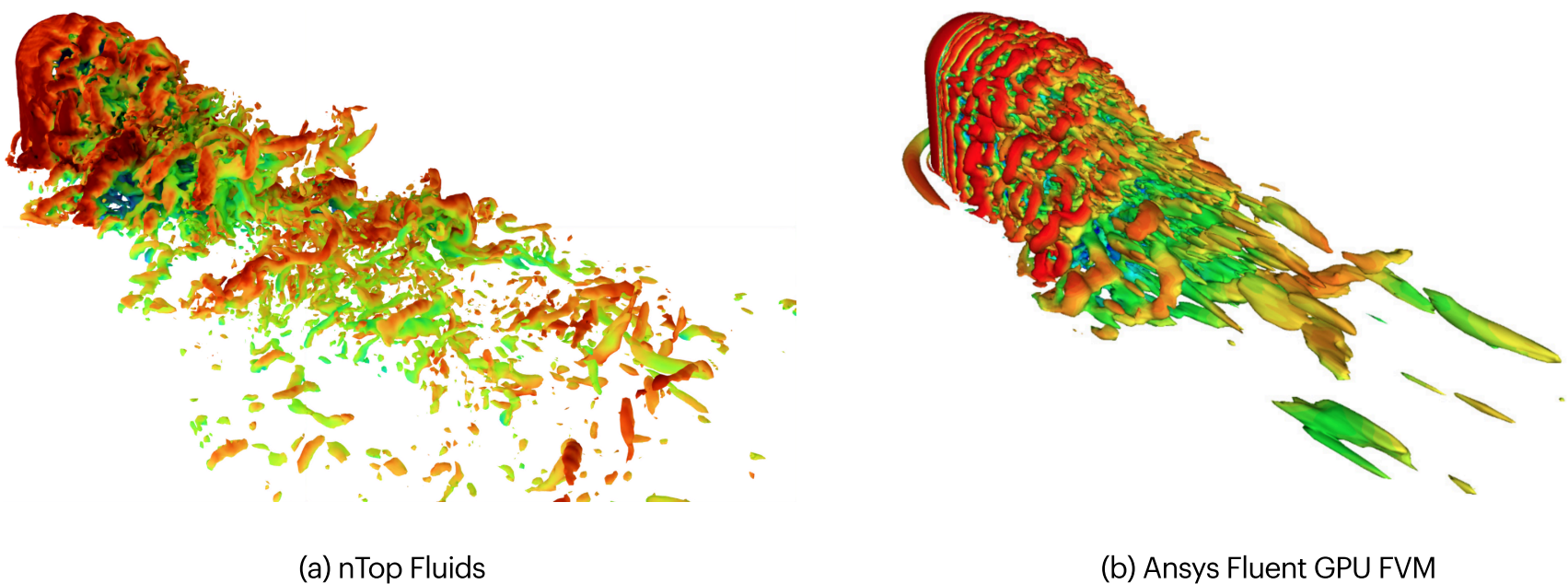


Figure 12: Turbulent wake flow structures colored by the velocity magnitude

The dimensionless pressure coefficient is given by

$$C_p = \frac{2(p - p_\infty)}{\rho u_\infty^2},$$

where p is static pressure at the probe position and p_∞ is static pressure in the freestream. In Figure 13, the 34 static pressure sensor locations on the side mirror surface are shown. Both solver's results are in good agreement

with the experimental data, see Figure 14. nTop is able to capture pressure coefficients with only marginal deviation from the experimental results in a number of surface probe locations. This indicates that nTop's simulation is able to capture a precise and comprehensive representation of the pressure distribution across the side mirror surface, reflecting its accuracy in capturing the aerodynamic details of the side mirror design.

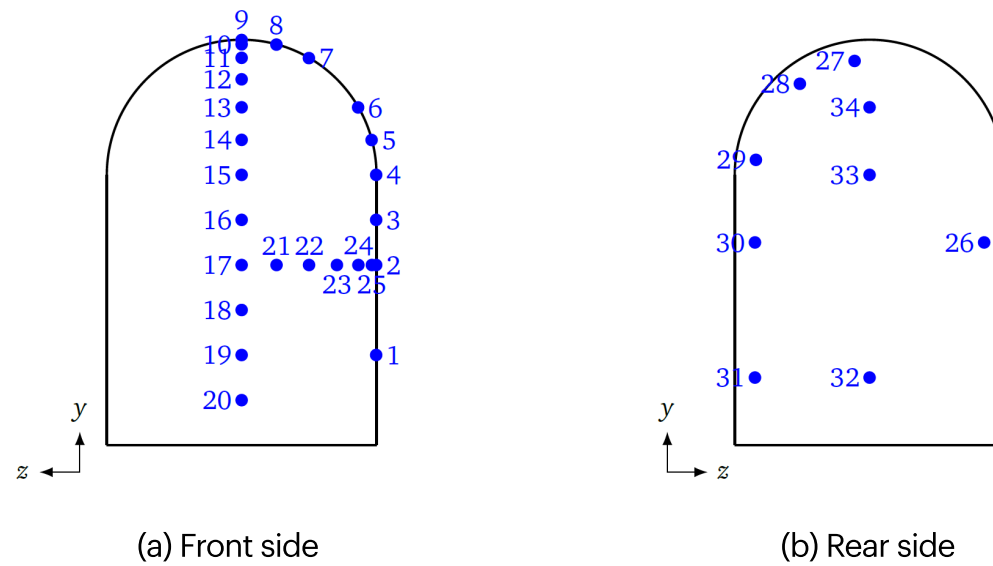


Figure 13: Probe locations of static pressure sensors over the front and rear side of the mirror

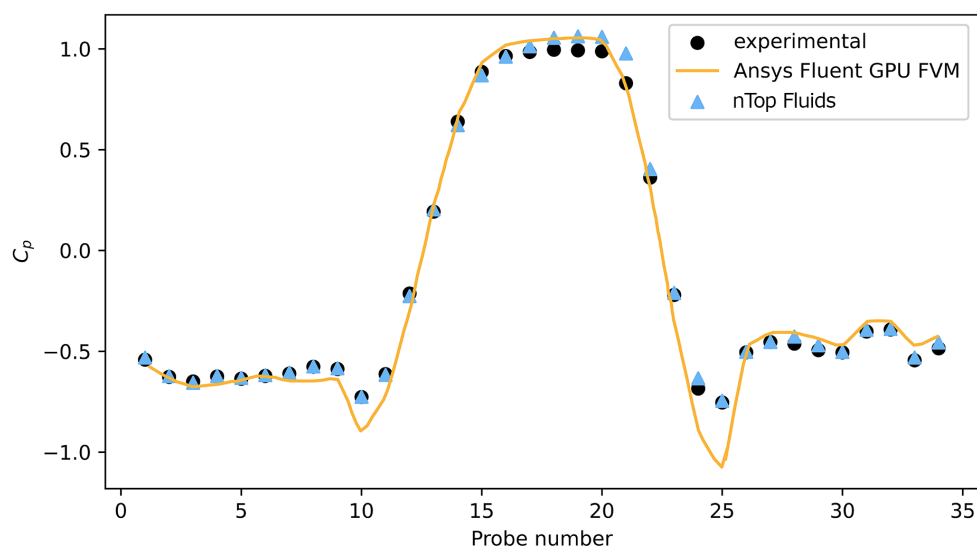


Figure 14: Pressure coefficient C_p values at the predefined sensor positions

Test case 5: FDA nozzle

In biomedical applications, where factors like temperature and biological conditions can influence results, reliable benchmarks are vital. The U.S. Food and Drug Administration (FDA) has proposed challenging benchmarks, including the idealized medical nozzle device, which has been utilized for Particle Image Velocimetry (PIV) measurements to provide reference standards for evaluating numerical solvers and experimental techniques [9]. In this study, we evaluate nTop and Ansys CFX [3] running on CPUs. By analyzing how each solver captures the transitional flow dynamics and measuring their computational efficiency against the PIV data, we aim to assess their effectiveness in replicating the complex flow characteristics of the nozzle. The nozzle dimensions are depicted in Figure 15, the flow direction for the sudden expansion configuration is from left to right. The used throat Reynolds number is defined as

$$\text{Re}_{\text{throat}} = \frac{u_{\text{mean}} d}{\nu} = 6500,$$

where u_{mean} is the mean velocity in the throat and d is the throat diameter.

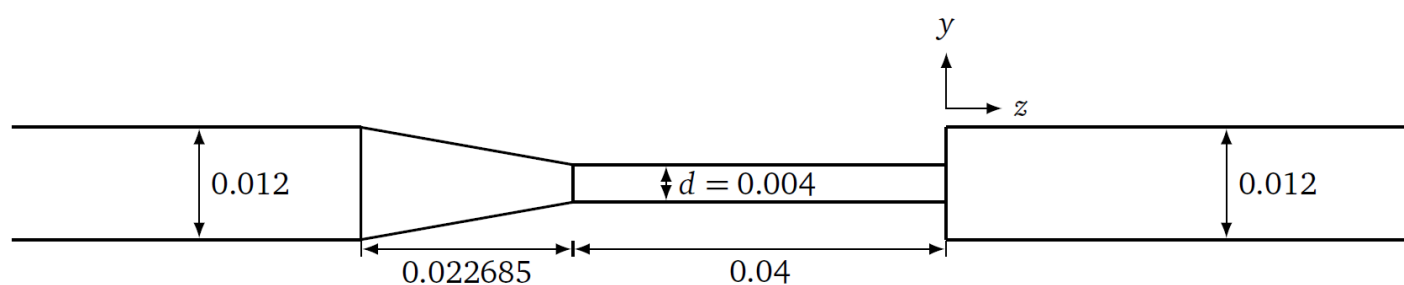
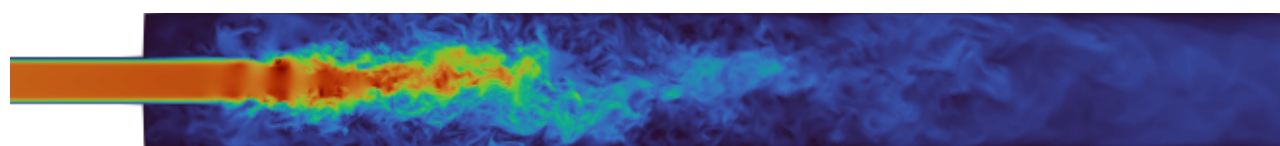
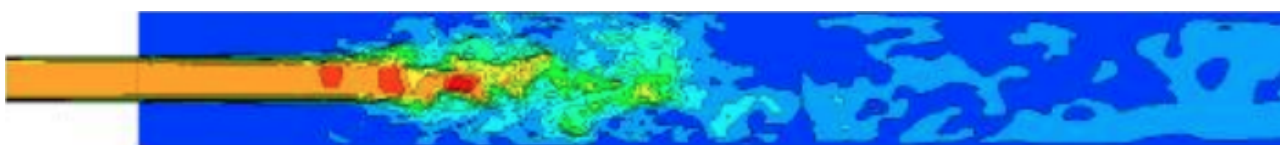


Figure 15: Geometrical dimensions of the FDA nozzle test case

In this study a Stress Blended Eddy Simulation (SBES) model with blended central difference (BCD) advection schemes is used in CFX and nTop again utilizes a WM-LES approach.



(a) nTop Fluids



(b) Ansys CFX CPU FVM [3]

Figure 16: Instantaneous velocity in the sudden expansion region

A qualitative comparison of the instantaneous velocity field in the sudden expansion region reveals notable differences between the two turbulence modeling approaches, see Figure 16. CFX's SBES model exhibits a longer jet throw distance and a later breakup of the jet compared to nTop's WM-LES. This indicates a more immediate transition to turbulence for the approach of nTop.

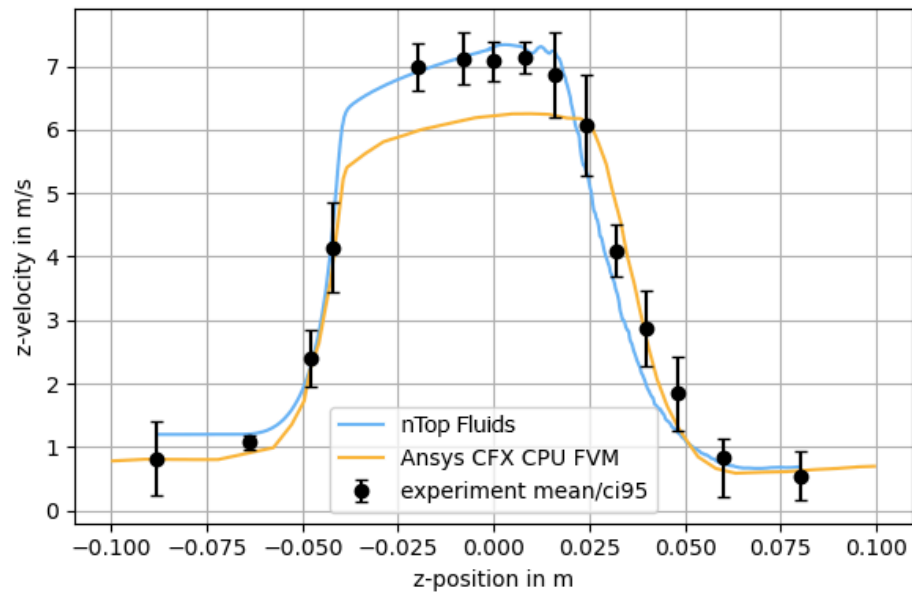


Figure 17: Axial velocity along nozzle centerline

In Figure 17, the axial velocity along the centerline of both solvers is compared to the experimental PIV data. The simulation results with CFX are unable to predict the velocity in the throat region ($z = -0.04 \dots 0.0\text{m}$) in the 95% confidence interval. The nTop results show a very good agreement in the throat region. At the jet breakup ($z = 0.025 \dots 0.05\text{m}$) CFX matches the experimental data closer and the nTop result falls within the confidence interval of the experimental data.

References

- [1] Ansys. Ansys Fluent Native Multi-GPU Solver: CFD Validation Studies in Version 23R2. Tech. rep. 2023.
- [2] Ansys. Speed AND Accuracy: First-Of-Its-Kind Broad-Spectrum CFD Solver Built Natively on GPUs. Tech. rep. 2022.
- [3] P. DREŠAR and J. DUHOVNIK. “A Hybrid RANS-LES Computational Fluid Dynamics Simulation of an FDA Medical Device Benchmark”. In: *Mechanics* 25.4 (2019), pp. 291–298.
- [4] R. Hold, A. Brenneis, and A. Eberle. “Numerical Simulation of aeroacoustic sound generated by generic bodies placed on a plate: Part-I, Prediction of aero acoustic sources”. In: *Proceedings of the 5th AIAA/CEAS Aeroacoustics Conference, 1999*. 1999.
- [5] K. Jain. “Efficacy of the FDA nozzle benchmark and the lattice Boltzmann method for the analysis of biomedical flows in transitional regime”. In: *Medical & biological engineering & computing* 58 (2020), pp. 1817–1830.
- [6] A. Kajzer and J. Pozorski. “Application of the Lattice Boltzmann Method to the flow past a sphere”. In: *Journal of Theoretical and Applied Mechanics* 55.3 (2017), pp. 1091–1099. ISSN: 1429-2955. DOI: 10.15632/jtam-pl.55.3.1091.
- [7] A. Sjunnesson, C. Nelsson, and E. Max. LDA measurements of velocities and turbulence in a bluff body stabilized flame. Dec. 1991.
- [8] D. M. Somers. “Design and experimental results for the S805 airfoil”. In: (Jan. 1997). DOI: 10.2172/437670.
- [9] S. F. Stewart, E. G. Paterson, G. W. Burgreen, P. Hariharan, M. Giarra, V. Reddy, S. W. Day, K. B. Manning, S. Deutsch, M. R. Berman, et al. “Assessment of CFD performance in simulations of an idealized medical device: results of FDA’s first computational interlaboratory study”. In: *Cardiovascular Engineering and Technology* 3 (2012), pp. 139–160.



199 Lafayette Street, Suite 4AB, New York, NY 10012

[Contact us](#)

